

**Letter of Intent: Searching for Muon
Neutrino Disappearance using
Mono-energetic Neutrinos from Kaon
Decay-at-rest at the J-PARC Materials
and Lifescience Facility**

December 14, 2015

M. Shaevitz

Columbia University, New York, New York, USA

S. Axani, G. H. Collin, J.M. Conrad, T. Wongjirad¹

Massachusetts Institute of Technology, Cambridge, Massachusetts, USA

J. Spitz

University of Michigan, Ann Arbor, Michigan, USA

¹Spokesperson: taritree@mit.edu

Executive Summary

Over the past two decades, several experiments have observed unexpected measured neutrino rates. These include an observed excess of $\bar{\nu}_e$ interactions measured in an accelerator-produced $\bar{\nu}_\mu$ source [1, 2], a ν_e excess in a ν_μ beam [3], and a set of $\bar{\nu}_e$ deficits seen in the flux of neutrinos coming from nuclear reactors [4, 5] and radioactive sources [6, 7, 8, 9]. One explanation for these anomalies is that neutrino oscillations are occurring between neutrinos with a mass splitting squared in the range 0.1 to 10 eV². These mass splittings, however, are several orders of magnitude larger than those measured from solar and atmospheric experiments. If the anomalies are truly from neutrino oscillations, the observations would be indicative of the existence of one or more neutrinos not included in the standard model. From measurements of the Z-boson width, there can only be three neutrinos that couple to the weak interactions. Therefore, these potential new neutrinos would not couple to any known force and are labeled as “sterile” neutrinos.

Besides confirming or refuting the anomalies directly, however, there is a complementary approach to probing the sterile neutrino oscillation hypothesis. The anomalies, if they are due to oscillations, fall into two categories: (anti-)muon-to-(anti-)electron flavor appearance and anti-electron flavor disappearance. However, muon flavor disappearance, which is required if the anomalies are due sterile flavor oscillations, has not been observed. In fact, global fits to the data indicate that the observation of muon-disappearance extends just beyond the limits set by past and current experiments.

We propose an experiment, “KPipe”, which will search for muon neutrino disappearance using monoenergetic (236 MeV) muon neutrinos coming from charged kaon decay-at-rest (KDAR) produced at the J-PARC Materials and Life Science Facility’s (MLF’s) spallation neutron source. The J-PARC MLF is the world’s most intense source of KDAR neutrinos, which provides a unique opportunity to perform a definitive search for muon disappearance consistent with the $\Delta m^2 \sim 1$ eV² anomalies, possibly indicative of one or more sterile neutrinos. The experiment would measure the rate of muon neutrino charged current quasi-elastic (CCQE) interactions along the length of a liquid scintillator detector 3 m in diameter and 120 m long, extending radially at a distance of 32 m to 152 m from the source. This formal proposal borrows much of its content from an informal published proposal and cost document [10, 11]

The proposed experiment contains a number of key features:

1. The neutrinos are mono-energetic and isotropic, making the flux in principle completely known.
2. The expected intrinsic background muon neutrino rate is extremely low: nearly 99% of CCQE interactions in the detector will be from KDAR neutrinos,
3. The signal CCQE interaction produces a distinct signature in the detector – a “double-flash” signal coming from the muon produced at the interaction vertex and its Michel electron – that when coupled with the pulsed beam from the J-PARC Rapid Cycling Synchrotron (RCS) allows for a high signal to background ratio;

4. By measuring the muon neutrino rate as a function of position along the detector, KPipe can trace out the oscillations as a function of distance, which would provide definitive evidence for (or against) sterile oscillations. It also provides data to determine the number of sterile neutrinos, if in fact they exist.

The required detector design, technology, and costs are modest. The KPipe measurements will be robust since they depend on a known energy neutrino source with low expected backgrounds. Further, since the measurements rely only on the measured rate of detected events as a function of distance, with no required knowledge of the initial flux and neutrino interaction cross section, the results will be largely free of systematic errors. The experimental sensitivity to oscillations, based on a shape-only analysis of the L/E distribution on six years of data, will extend an order of magnitude beyond present experimental limits in the relevant high- Δm^2 parameter space. Such a search for muon neutrino disappearance would complement searches for $\bar{\nu}_e$ appearance, such as JSNS². If a sterile neutrino exists, together their results would provide a complete and consistent picture of sterile neutrino oscillations, all coming from the J-PARC MLF.

Contents

1	Physics Motivation	5
2	The KDAR source and KPipe Detector	6
3	Simulation of the Experimental Setup	10
4	Isolating and Reconstructing ν_μ Events from the KDAR Source	14
4.1	Isolating the Signal	15
4.2	Detection efficiency	18
5	Sensitivity	19
5.1	KPipe sensitivity versus past results and future experiments	21
6	Cost Estimate	22
6.1	Vessel	23
6.2	Scintillator	24
6.3	Photon detectors and Readout Electronics	24
6.4	Facilities	24
6.5	Cost Summary for Detector	25
7	Estimated Schedule	25
8	Conclusion	26

1 Physics Motivation

A number of experimental anomalies consistent with neutrino oscillations at a characteristic mass splitting around 1 eV^2 hint at the possibility of an additional neutrino. These anomalies fall into two categories: muon-to-electron flavor appearance, as observed by the LSND [1] and MiniBooNE [3, 2] experiments, and electron flavor disappearance, as observed by reactor [4, 5] and source [6, 7, 8, 9] experiments. A favored beyond-Standard-Model explanation for these anomalies invokes an additional number of N sterile neutrinos participating in oscillations beyond the three active flavors [12, 13, 14, 15]. These “3+ N models” are able to simultaneously describe the existing anomalous observations and those measurements which do not claim a signal in the relevant parameter space [16, 17, 18, 19, 20, 21, 22, 23, 24], although there is tension between both neutrino and antineutrino measurements and appearance and disappearance measurements.

Muon neutrinos, for example, must disappear if the observed anomalies are due to oscillations involving a light sterile neutrino. The lack of observed ν_μ disappearance is a major source of tension in the global fits. In order to understand the importance of ν_μ disappearance measurements, consider a 3+1 sterile neutrino model, with the probability for $\nu_\mu \rightarrow \nu_e$ appearance given by:

$$P(\nu_\mu \rightarrow \nu_e) \simeq 4|U_{\mu 4}|^2|U_{e 4}|^2 \sin^2(1.27\Delta m_{41}^2 L/E) . \quad (1)$$

The probability for ν_e and ν_μ disappearance are, respectively:

$$P(\nu_e \rightarrow \nu_e) \simeq 1 - 4(1 - |U_{e 4}|^2)|U_{e 4}|^2 \sin^2(1.27\Delta m_{41}^2 L/E) \quad (2)$$

and

$$P(\nu_\mu \rightarrow \nu_\mu) \simeq 1 - 4(1 - |U_{\mu 4}|^2)|U_{\mu 4}|^2 \sin^2(1.27\Delta m_{41}^2 L/E) . \quad (3)$$

In these equations, the elements of the mixing matrix, U , set the amplitude of oscillation, while Δm_{41}^2 establishes the oscillation wavelength. Within this 3+1 model, a global fit to the world’s data, including all anomalies and null results, will simultaneously constrain $U_{e 4}$, $U_{\mu 4}$, and Δm_{41}^2 . The range of values that $U_{\mu 4}$ can take on, and therefore the oscillation parameters that govern ν_μ disappearance, can thus be restricted. The present global fit for ν_μ disappearance places the allowed region just outside of current bounds. This motivates the construction of a fast, low cost, and decisive ν_μ disappearance experiment that can confirm or disallow various models for sterile neutrinos, as well as inform a range of future proposed experiments [25, 26, 27, 28, 29, 30, 31, 32, 33, 34].

In what follows² we describe such an experiment, called “KPipe”, that can perform a search for ν_μ disappearance that extends well beyond current limits while still being low cost. KPipe will employ a long, liquid scintillator-based detector that is oriented radially with respect to an intense source of monoenergetic 236 MeV ν_μ s coming from the decay-at-rest of positively charged kaons ($K^+ \rightarrow \mu^+ \nu_\mu$; BR=63.55±0.11% [35]). As the only relevant monoenergetic neutrino that can interact via the charged current interaction, a kaon decay-at-rest (KDAR) ν_μ source represents a unique and important

²Much of this document borrows from our paper, Phys. Rev. D 92, 092010.

tool for precision oscillation, cross section, and nuclear physics measurements [36, 37]. Since the energy of these neutrinos is known, indications of ν_μ disappearance may be seen along the length of the KPipe detector as oscillating deviations from the expected $1/R^2$ dependence in the rate of ν_μ charged-current (CC) interactions. A measurement of such a deviation over a large range of L/E would not only be a clear indication for the existence of at least one light sterile neutrino, but also begin to disambiguate among different sterile neutrino models.

2 The KDAR source and KPipe Detector

The Materials and Life Science Experimental Facility (MLF) at the Japan Proton Accelerator Research Complex (J-PARC) in Tokai, Japan houses a spallation neutron source used for basic research on materials and life science, as well as research and development in industrial engineering. It is also an intense, yet completely unutilized, source of neutrinos that emits the world’s most intense flux of KDAR monoenergetic (236 MeV) ν_μ s. Neutron beams along with neutrinos are generated when a mercury target is hit by a pulsed, high intensity proton beam from the J-PARC rapid-cycling synchrotron (RCS) [30]. The RCS delivers a 3 GeV, 25 Hz pulsed proton beam, which arrives in two 80 ns buckets spaced 540 ns apart. The facility provides users 500 kW of protons-on-target (POT) but has demonstrated its eventual steady-state goal of 1 MW, albeit for short times [38]. Along with neutrons and muons, the proton-on-target interaction provides an intense source of light mesons, including kaons and pions, which have a large branching ratio to ν_μ s. The produced kaons usually come to rest in the high-A target and surrounding shielding, providing a high-intensity source of monoenergetic ν_μ s.

KPipe will search for muon-flavor disappearance with CC interactions of 236 MeV ν_μ s on carbon nuclei ($\nu_\mu {}^{12}\text{C} \rightarrow \mu^- X$) in liquid scintillator. This interaction produces a visible muon and X , where X is some combination of an excited nucleus, de-excitation photons, and one or more ejected nucleons after final state interactions. The goal of the KPipe detector design is to efficiently identify these 236 MeV ν_μ CC events, broadly characterized by two separated flashes of light in time coming from the prompt $\mu^- X$ followed by the muon’s decay electron.

The KPipe design calls for a relatively low cost, 3.0 m inner diameter steel-reinforced, high-density polyethylene (HDPE) pipe that is filled with liquid scintillator. As shown in Fig. 1, the pipe is positioned so that it extends radially outward from the target station. The upstream location maximizes the sensitivity to oscillations by being the shortest possible distance from the source, given spatial constraints. We have found that a long detector (120 m, 684 tons) is most suitable for optimizing sensitivity to oscillations across a wide range of the most pertinent parameter space, in consideration of current global fit results, the neutrino energy, $1/R^2$, and estimated cost.

The interior of the pipe contains a 2.8 m diameter, stainless-steel cylinder of highly reflective panels, which optically separate the target volume (inner detector) from the cosmic ray (CR) veto (outer detector). Hoops of inward-facing silicon photomultipliers (SiPMs) are mounted on the interior of the panels. There are 100 equally-spaced

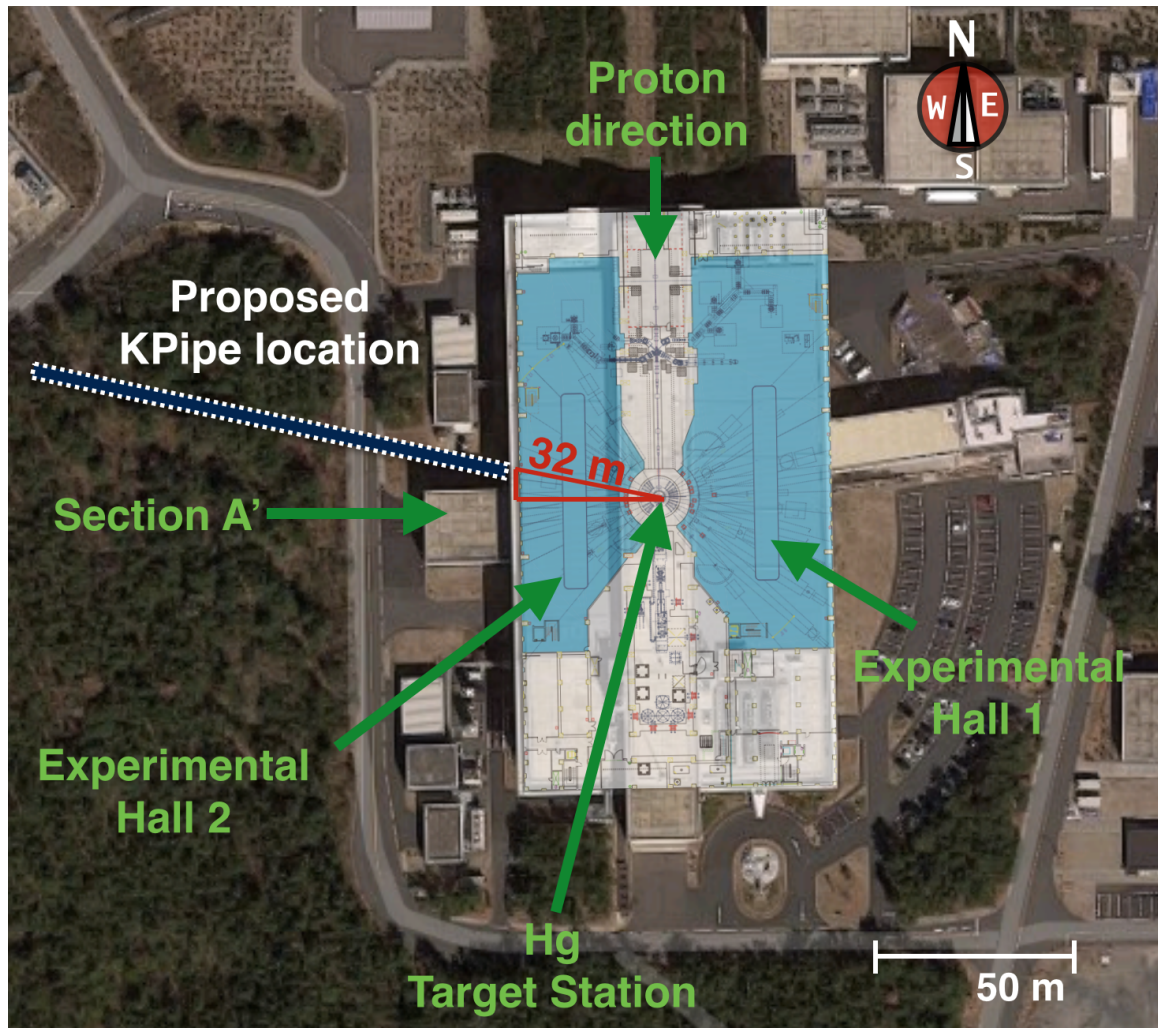


Figure 1: An aerial view from Google Maps (2015) of the Materials and Life Science Facility layout with a superimposed schematic drawing [30] of the first floor, including the target station. The proposed KPipe location (shown with a dotted contour) is 32 m from the target station and 102° with respect to the incident proton beam direction. The detector extends radially outward from the target station.

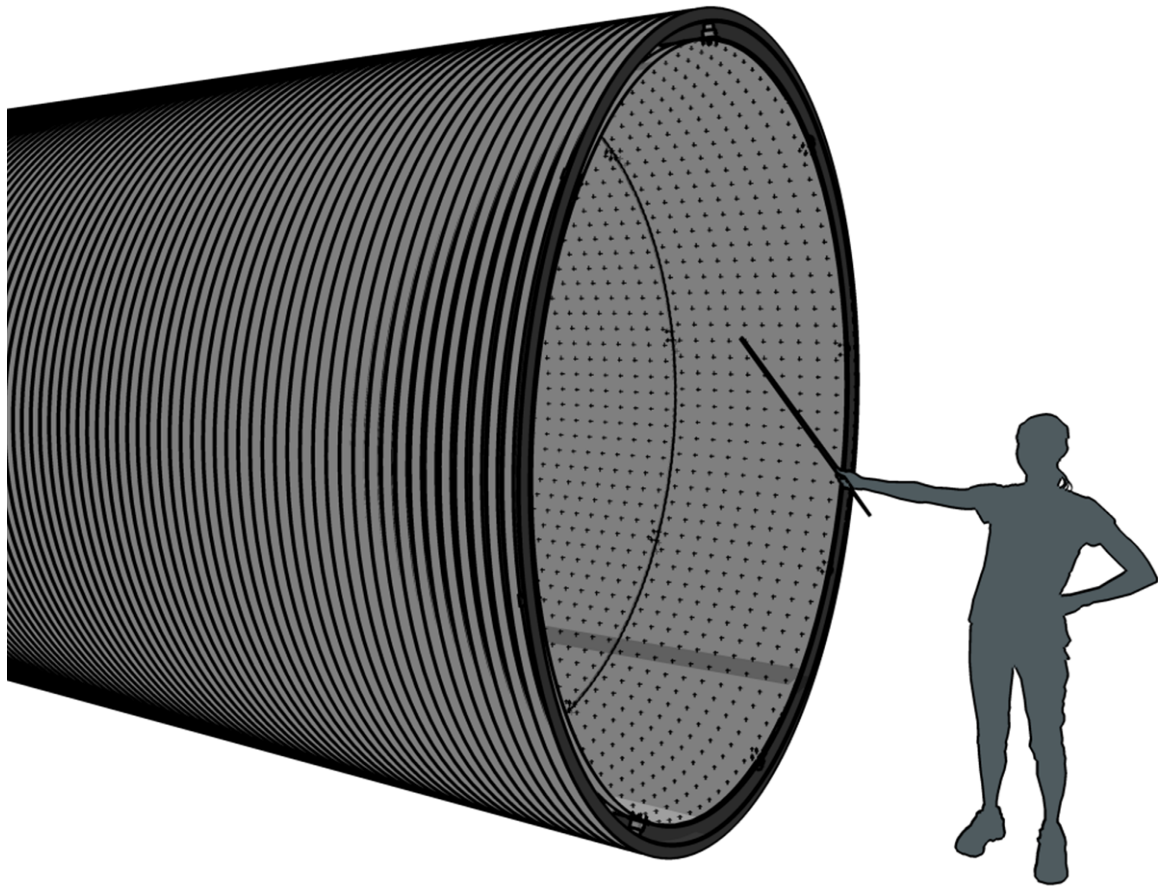


Figure 2: The KPipe detector design, featuring a 3.0 m inner diameter high density polyethylene (HDPE) vessel filled with liquid scintillator. Silicon photomultipliers (SiPMs) are seen mounted on the interior panels in hoops spaced by 10 cm in the longitudinal direction. The cosmic ray veto is a 10 cm space between the panels and the outer HDPE wall.

SiPMs per hoop, and each hoop is separated longitudinally by 10 cm (see Fig. 2). The space surrounding the inner target region on the other side of the panels is the 10 cm-thick veto region. The surfaces of the veto region are painted white, or lined with a Tyvek[®]-like material, for high reflectivity. Along the innermost side of the veto region are 120 hoops of outward-facing SiPMs that each run along the circumference of the pipe. The hoops have 100 SiPMs each and are positioned at 1 m spacing along the inside of the veto region. The 10 cm spaces at the ends of the pipe are also instrumented. Each veto end cap is instrumented with 100 SiPMs that all face axially outward and are spaced equally apart on a circle with 1 m radius.

SiPMs are employed in both the target and veto regions because of their compact size and reduced cost when purchased in bulk. Currently available SiPMs typically have a quantum efficiency around 30%. In order to further reduce cost, we plan on multiplexing the SiPM channels. For the target region, each channel of readout electronics monitors 25 out of the 100 total SiPMs on a hoop. For the veto region, one channel monitors one side or end cap hoop. The active area of a SiPM can range from 1 mm² to about 6 mm². Assuming 6 mm² SiPMs, with 1200 hoops containing 100 SiPMs each, the target region will have a photocathode-coverage of only $\sim 0.4\%$. Despite this low coverage, simulations of the experiment described in the next section indicate that there are an adequate number of SiPMs to achieve the goals of the experiment.

The KPipe detector succeeds despite the sparse amount of instrumentation in the inner region because of its use of liquid scintillator as the detector medium. The low photocathode coverage is overcome by the large amount of light produced by the scintillator per unit of energy deposited. Scintillators under consideration for KPipe include those based on mineral oil and linear alkylbenzene (LAB). One example of a currently-deployed mineral oil-based scintillator is the one used by the NO ν A experiment [39]. This scintillator is a mixture of 95%-by-mass mineral oil with 5% pseudocumene (1,2,4-trimethylbenzene) along with trace amounts of PPO (2,5-diphenyloxazole) and bis-MSB (1,4-Bis(2-methylstyryl)benzene) wavelength shifters [40]. The UV photons emitted by the pseudocumene excite the PPO, which, as the primary scintillant, re-emits in the range of 340-380 nm. These photons are then absorbed by the bis-MSB and reemitted in the 390-440 nm range. Along with developing their scintillator, the NO ν A experiment has also established the methods to manufacture large quantities of it at a relatively low cost. Other examples of mineral oil-based scintillators are those offered by Saint-Gobain. For reference, the light yield of these scintillators range from 28% to 66% of anthracene or ~ 4500 to ~ 11400 photons/MeV [41]. Besides mineral oil, another option is to use a LAB-based liquid scintillator, similar to that being used by the SNO+ experiment [42]. This liquid scintillator consists of the LAB solvent with PPO acting as the wavelength shifter. The advantage of a LAB-based liquid scintillator over those based on mineral oil is that it has a comparable light yield to the brighter Saint-Gobain scintillators [43] while also being less toxic. In order to be conservative, we assume in simulations of the KPipe detector (discussed in the next section) a light yield consistent with the dimmest mineral oil based liquid scintillator from Saint-Gobain (4500 photons/MeV). The liquid scintillator that is eventually employed for KPipe will be some optimization between light yield, cost, and safety.

3 Simulation of the Experimental Setup

In order to study the performance capabilities of KPipe, we have created simulations of both the neutrino source and the detector. The source simulations, using both Geant4 [44] and MARS15 [45], model 3 GeV kinetic energy protons hitting the mercury target. The resulting particles are propagated, and the kinematics of all the neutrinos produced are recorded. A semi-realistic geometry, which includes a simplified model of the Hg target, H₂O moderator, Be reflector, and Fe shielding, is employed with Geant4 for the target and surrounding material, although the majority (86%) of 236 MeV ν_μ are found to originate within the mercury target. About 75% of the K^+ are found to DAR within 25 cm of the upstream end of the mercury target and the ratio of ν_μ from K^+ DAR to ν_μ from K^+ decay-in-flight over 4π is $\sim 13:1$. The K^+ production rate varies depending on which simulation software is used. The Geant4 model calculates the 236 MeV ν_μ yield to be 0.0038 ν_μ per proton on target (POT), whereas the MARS15 model predicts 0.0072 ν_μ /POT. Later, when calculating the sensitivity of the experiment in Section 5, we will quote a sensitivity which relies on the MARS15 model for kaon production, as it has been more extensively tuned to data than Geant4 [46].

The ν_μ flux is propagated to the KPipe detector whose closest end to the source is 32 m away. The ν_μ flux for $-0.25 < \cos \theta_z < -0.16$, where θ_z is the neutrino angle with respect to the proton direction ($+z$), representative of the full detector length, is shown in Fig. 3 (left). The time distribution of all neutrinos coming from the source is shown in Fig. 3 (right). The two 80 ns wide proton pulses can be seen in the figure, while the blue histogram shows the neutrinos coming from kaon decay.

The interactions of neutrinos with the detector target and surrounding materials are modeled with the NuWro event generator [47], and the ν_μ CC cross section and expected rate can be seen in Fig. 4. Notably, the signal (KDAR) to background (non-KDAR) ratio is 66:1 integrated over all energies. In other words, if a neutrino-induced muon is observed, there is a 98.5% chance that it came from a 236 MeV ν_μ CC interaction. Given 5000 hours/year of J-PARC 1 MW operation (3.75×10^{22} POT/year), consistent with Ref. [48], we expect 1.02×10^5 KDAR ν_μ CC events/year in the 684 ton active volume.

For each generated 236 MeV ν_μ CC interaction on carbon, NuWro provides the momentum of the outgoing muon and any final state nucleons (typically a single proton). Fig. 5 shows the kinetic energies of the resulting KDAR signal muons along with the non-KDAR muons. The ν_μ CC cross section on carbon at 236 MeV according to NuWro and employed for the event rate estimate here is 1.3×10^{-39} cm²/neutron. This is consistent with the Random Phase Approximation (RPA) model's [49, 50, 51] cross section prediction of $(1.3 + 0.2) \times 10^{-39}$ cm²/neutron (RPA QE+nph). While NuWro is the only generator we use to produce simulated events, we did compare the kinematic distributions given by NuWro to that provided by GENIE [52] and the Martini *et al.* RPA model [51], which includes multi-nucleon effects. We find that the difference in the muon kinematic predictions among the models is not large enough to significantly change the detector simulation and oscillation sensitivity results.

Particle propagation through the detector is modeled using the Geant4-based simulation package RAT [53]. The detector geometry input into the simulation is as

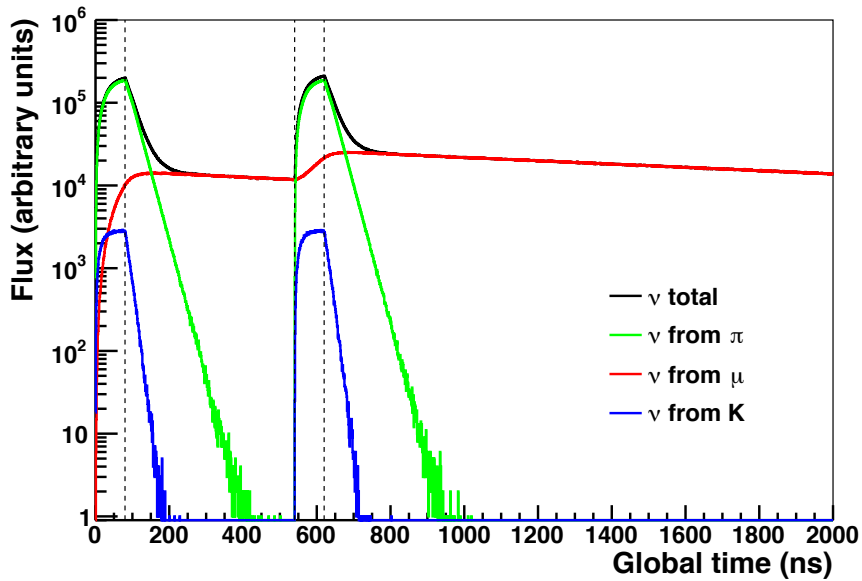
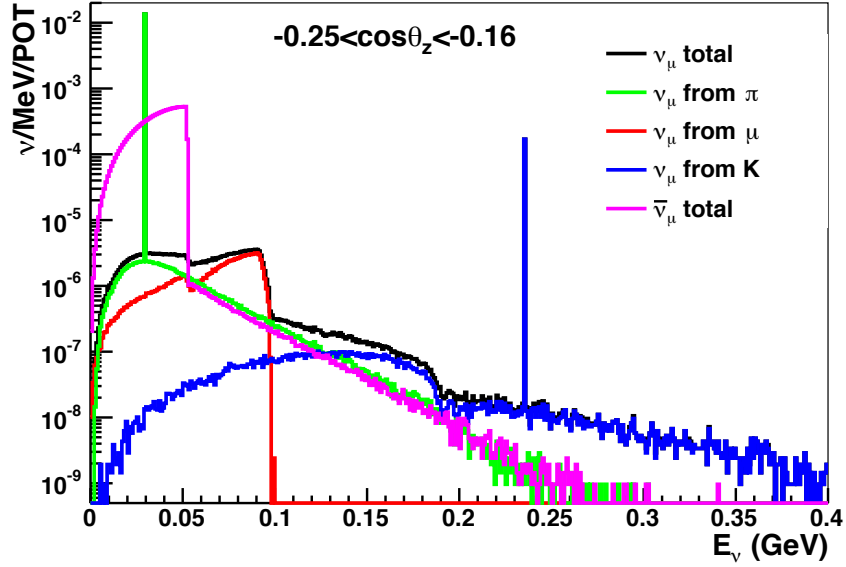


Figure 3: Top: The muon neutrino and antineutrino flux with $-0.25 < \cos\theta_z < -0.16$, representative of the full detector length, where θ_z is the neutrino angle with respect to the proton direction ($+z$). Bottom: The neutrino creation time relative to the two beam pulses (dotted lines). This distribution includes neutrinos emitted over all solid angles and energies.

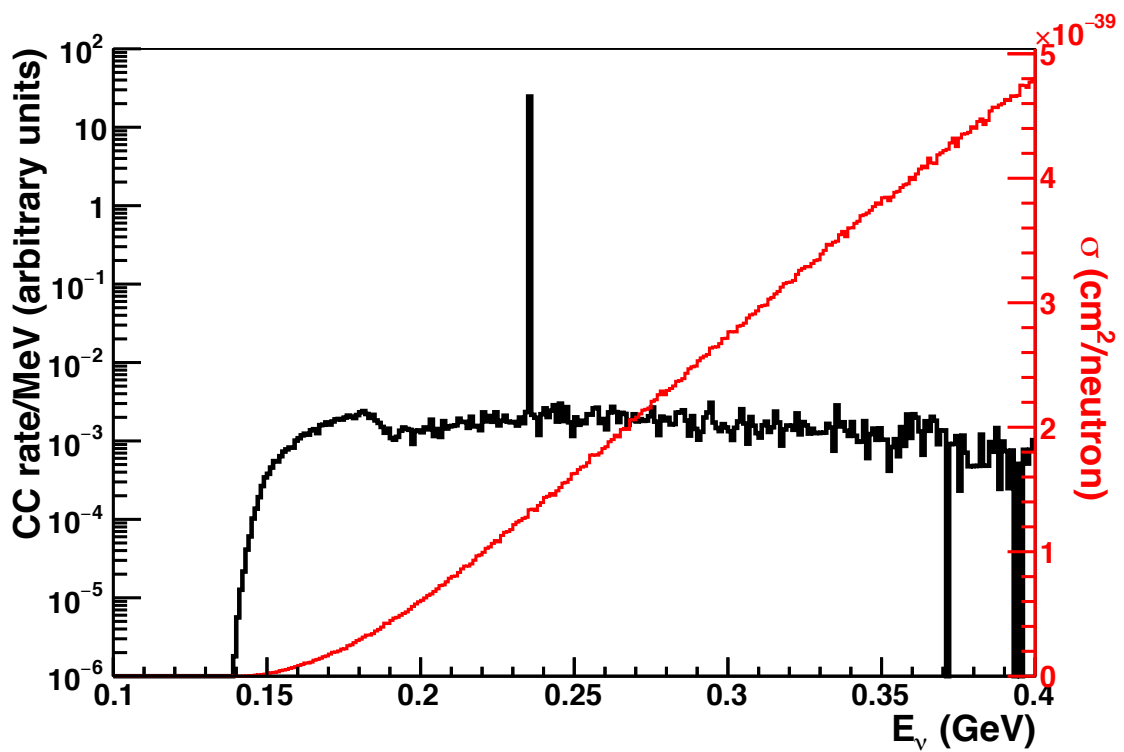


Figure 4: The ν_μ charged current event rate, for neutrinos with $-0.25 < \cos \theta_z < -0.16$, along with the employed ν_μ CC cross section. The monoenergetic 236 MeV neutrino signal is clearly visible above the “background” non-monoenergetic events, mainly coming from kaon decay-in-flight.

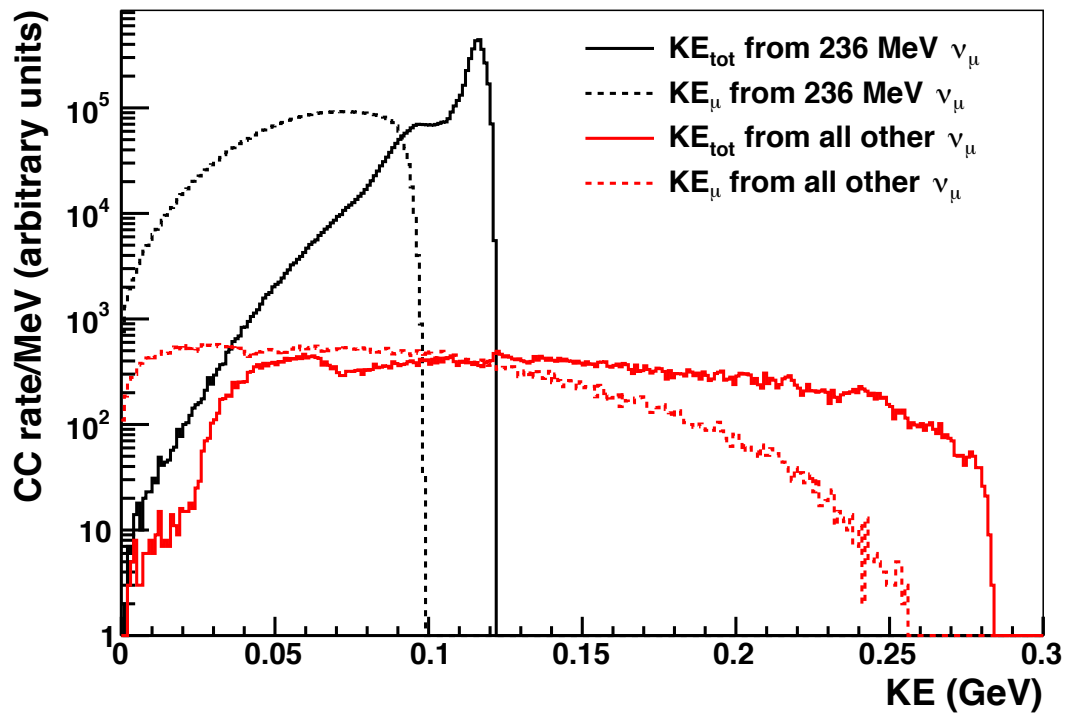


Figure 5: The muon and total kinetic energy ($KE_{\text{tot}} = KE_{\mu} + \sum KE_p$) for the signal 236 MeV ν_{μ} charged current events compared to all other ν_{μ} . Only neutrinos with $-0.25 < \cos\theta_z < -0.16$ are considered. The ratio of integrated signal (black) to background (red) is 66:1.

described in the previous section. The detector is assumed to be on the surface and is surrounded by air only. Neutrino events are distributed over a 5 m x 5 m x 140 m box that fully contains the 120 m long, 3.0 m diameter cylindrical detector. The distribution of events in the box is weighted to take into account the $1/R^2$ dependence of the flux along with the density of the various materials in the simulation. The small divergence in the neutrino direction is also considered. The RAT package includes a model for scintillator physics that derives from models previously employed by other liquid scintillator experiments such as KamLAND. The processes that are considered include scintillation, absorption, and reemission. All three have wavelength dependence. The reflectivity of surfaces in the detector is simulated using the models built into Geant4.

In addition to the simulation of KDAR neutrino interactions with the detector and surrounding material, we simulated the propagation of CR throughout the volume. We used the simulation package CRY [54] to study the CR particle flux, which generates showers consisting of some combination of one or more muons, pions, electrons, photons, neutrons, or protons. The dark rate of SiPMs is also included in the simulation of the SiPM response. We use a dark rate of 1.6 MHz for each of the 130,200 4 mm x 4 mm SiPMs (0.4% photo-coverage) along with a total quantum efficiency of 30%. The dark rate comes from the specification for SenSL series C SiPMs which have an advertised dark rate of $< 100,000$ Hz/mm² [55].

4 Isolating and Reconstructing ν_μ Events from the KDAR Source

Signal events from the KDAR neutrino source are identified by the observation of two sequential pulses of light. The first pulse comes from the muon and vertex energy deposition. The next signal is from the Michel electron produced by the decay of the muon ($\nu_\mu^{12}\text{C} \rightarrow \mu^- X, \mu^- \rightarrow e^- \nu_\mu \bar{\nu}_e$). We apply a pulse finding algorithm to identify both light signals from the SiPMs. The algorithm uses a rolling 20 ns window over which the number of hits in the SiPMs are summed and the expected dark hit contribution in the window is subtracted. The first pulse is found when the hit sum with subtraction is above a given threshold, specifically one that is four times larger than the standard deviation of the expected number of dark hits. After the first pulse is found, the algorithm searches for the Michel signal using the same method, except that the threshold is raised to account for both the expected dark noise and the contribution of SiPM hits from the first pulse. This expected hit contribution is dictated by the decay time of the scintillator. After isolating coincident signals, the position along the detector of both the primary interaction and Michel signal is determined by the photoelectron-weighted position of the hits seen by the SiPMs. Using the position of the prompt pulse, we find that the vertex position resolution of the interaction is 80 cm. The current proposed readout is likely unable to reconstruct more detailed information about the event such as the muon angle, although this information is not necessary for KPipe's primary measurement.

Fig. 6 shows the number of photoelectrons (pe) in the first pulse as a function of

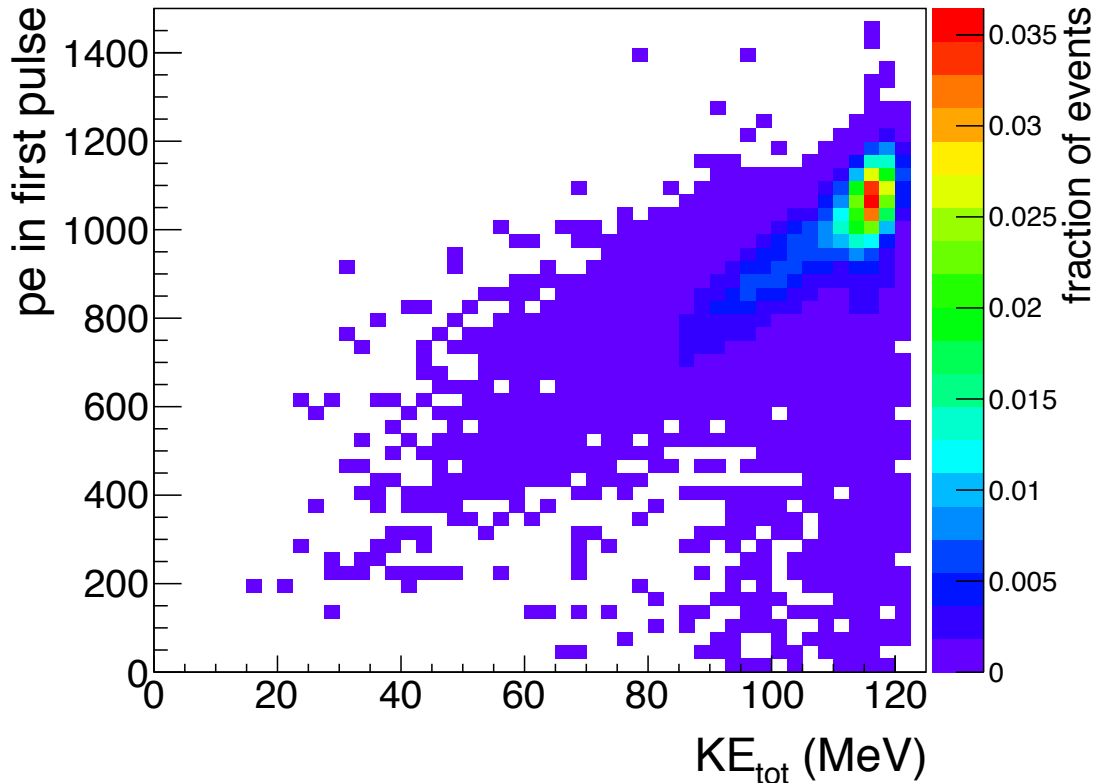


Figure 6: The number of photoelectrons in a 236 MeV ν_μ CC event's first pulse versus the total kinetic energy ($KE_{\text{tot}} = KE_\mu + \sum KE_p$).

total kinetic energy, KE_{tot} , defined as the total kinetic energy of the muon and any final state protons ($KE_{\text{tot}} = KE_\mu + \sum KE_p$). The figure shows simulated data from KDAR ν_μ CC interactions. The first pulse usually contains over 800 pe , indicating that, despite the low photocathode coverage, the amount of observed light for the signal events is high enough for efficient reconstruction. Further, the figure shows that KE_{tot} correlates well with the number of pe seen. Using the peak of this distribution, the detector light yield is calculated to be 9.2 pe/MeV , which includes effects from quantum efficiency, photocathode-coverage, and absorption.

4.1 Isolating the Signal

The primary background to the ν_μ CC signal events comes from stopping cosmogenic muons in the detector. We envision applying the following selection requirements in order to select signal interactions and reject CR backgrounds:

1. the first interaction signal (detected muon) occurs within 125 ns windows following each of the two 80 ns beam pulses,
2. the interaction signal has a reconstructed energy in the range $22 < E_{\text{vis}} < 142$ MeV ($200 < pe < 1300$),

3. the Michel signal occurs within $10 \mu\text{s}$ of the interaction signal,
4. the Michel signal reconstructed visible energy is $11 < E_{\text{vis}} < 82 \text{ MeV}$ ($100 < pe < 750$),
5. the distance between the interaction signal and the Michel signal is less than 1.5 m , and
6. the summed pulse height in the veto SiPMs is less than four times the dark rate σ within a 125 ns window after the start of each 80 ns beam pulse.

Note that for the cuts on visible energy, E_{vis} , the corresponding values in pe are given in parentheses. These are the values used in the Monte Carlo study of the KDAR signal efficiency and CR background rejection.

The first cut (1) takes advantage of the pulsed proton beam. Accepting events only within a 125 ns window after each 80 ns proton pulse efficiently selects 99.9% of the KDAR neutrinos while removing many of the events coming from other neutrino sources. The small 125 ns event window also limits the rate of CR ray events even before the other selection cuts are applied. According to the simulation, CR particles create at least one detectable flash in either the target region or veto in only 0.87% of all windows.

The second cut (2) utilizes the fact that, because the signal events come from monoenergetic neutrinos, the energy of the outgoing particles falls in a fairly narrow range. Fig. 7 shows the total kinetic energy of the muons and any final state protons, KE_{tot} , as a function of neutrino energy for ν_{μ} CC events in the detector. The upper bound of 142 MeV ensures that the signal neutrino events are preserved with high efficiency, while removing non-KDAR muon neutrinos at higher energies. More importantly, the upper bound removes bright CR events. Based on the simulation, 72% of all detectable CR events (i.e. ones that produce one or more detected flashes) are removed by the high energy cut, many of which are through-going muons. Along with kaon decay-in-flight neutrinos, the low energy bound also removes all relevant backgrounds from CR-induced spallation products and is well above the visible energy from radiogenic backgrounds. With both a high and low energy cut on the first pulse, 87% of all CR events are removed.

The cuts related to Michel electron timing, energy, and spatial coincidence (cuts 3-5) are chosen to efficiently retain signal while removing most of the in-time through-going CR muons that traverse the detector, as well as other backgrounds. A coincident signal coming from non-stopping muons can occur due to a CR shower with two or more particles or an associated muon spallation-induced isotope. The timing, energy, and spatial cuts on the Michel candidate reduce much of this coincident background. Applying the above cuts along with the Michel pulse cuts reduces the CR rate to 750 Hz , which means that only 0.01% of all signal windows will contain a CR event. At this stage in the cuts, less than two percent of detectable CR events remain.

The final cut (6) applied removes all events that create a flash of light in the veto. The veto is only 10 cm thick and is more sparsely instrumented than the target region. However, enough light is produced that the veto is able to reject 99.5% of all detectable CR events with at least one muon. We find that lining the walls of the

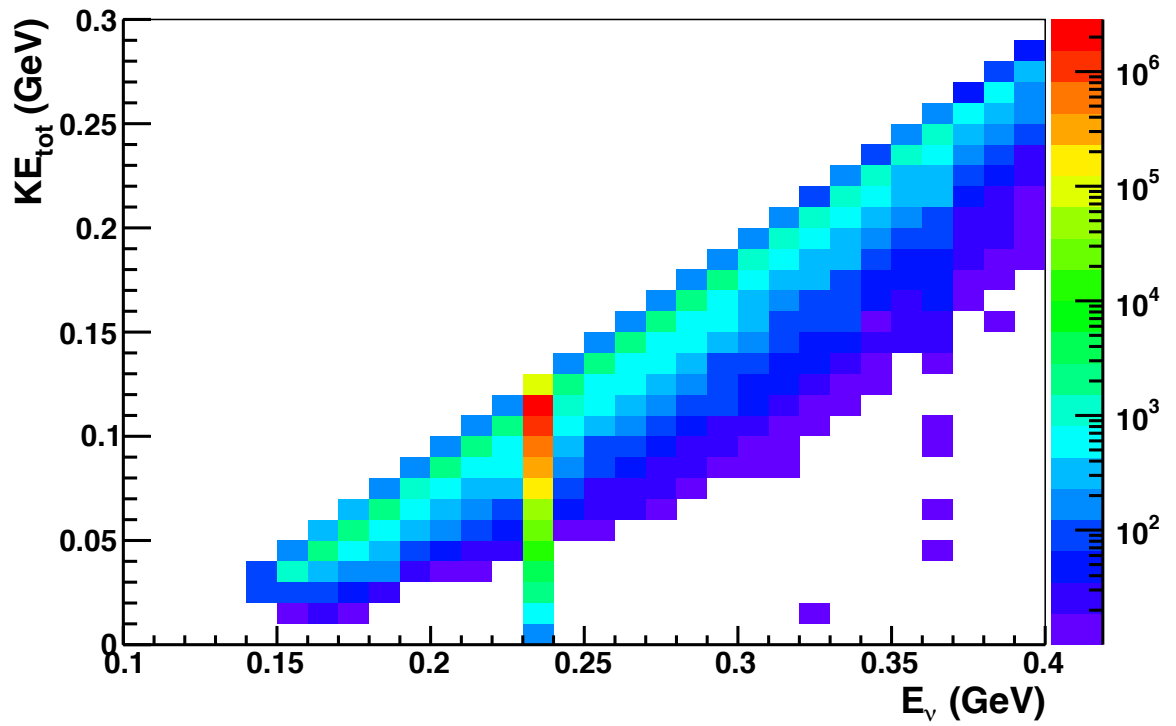


Figure 7: The total kinetic energy ($KE_{\text{tot}} = KE_\mu + \sum KE_p$) versus the energy of neutrinos from CC interactions in KPipe. Only neutrinos with $-0.25 < \cos \theta_z < -0.16$ are considered. The Z-axis units are arbitrary.

veto with a highly reflective material plays an important role in the veto performance. With all cuts applied, we estimate that the rate of CR events is 27 Hz over the entire fiducial volume.

In addition to CR backgrounds and non-KDAR muon neutrino events, an additional coincident background can come from beam-induced neutron interactions that produce a Δ^+ in the detector that subsequently decays into a π^+ . The latter can then stop and decay to a muon followed by a Michel electron. We assume that this background is negligible for this study. All in-time beam-related backgrounds will be measured before deploying KPipe, and adequate shielding will be installed in order to mitigate them.

Overall, our studies indicate that the dominant background is from CR shower events that are not removed by the above cuts. Of the 27 Hz rate that passes, the simulations show that 68% of the rate is due to stopping muons. The remaining 32% is due to showers involving photons, electrons, and neutrons. In the simulation, we do not include any additional passive shielding, for example coming from overburden. If the detector is buried or shielded, we expect these non-muon backgrounds to be further reduced. The CR background should be distributed uniformly throughout the detector and can be measured precisely using the identified out-of-time stopped muons. As a result, only the statistical error from the total number of background events expected to pass the cuts is included in the sensitivity analysis, described later in Section 5.

4.2 Detection efficiency

The cuts introduce inefficiency in the signal. We assume that the neutrino events are distributed evenly in radius and fall as $1/R^2$ throughout the detector. Signal events near the lateral edge of the target region can exit the detector before the muon can decay. This leads to an acceptance that is a function of radius. Based on a fiducial radius of 1.45 m, we find an acceptance of 87% with respect to KDAR ν_μ CC interactions whose true vertex is in the target region. The selection cuts described above are 89% efficient according to the simulation. This includes events where the muon is captured by the nucleus, which occurs in the target region 6% of the time. For a subset of these events, there is also an additional 0.75% dead-time loss due to the rate of CR events in the veto.

In summary, the total efficiency for all signal events is 77%, leading to an expected total KDAR ν_μ CC rate of 7.8×10^4 events distributed along the pipe's fiducial volume per year of running. This is on average 4.9×10^{-5} KDAR events per proton beam window without oscillations. This compares with 3.4×10^{-6} CR events per proton beam window. At the end of the pipe nearest the source, the unoscillated signal to background ratio in the number of events in the first 1 m of the detector is about 60:1. At the furthest end of the pipe, the unoscillated signal to background ratio in the last 1 m of the detector is about 3:1.

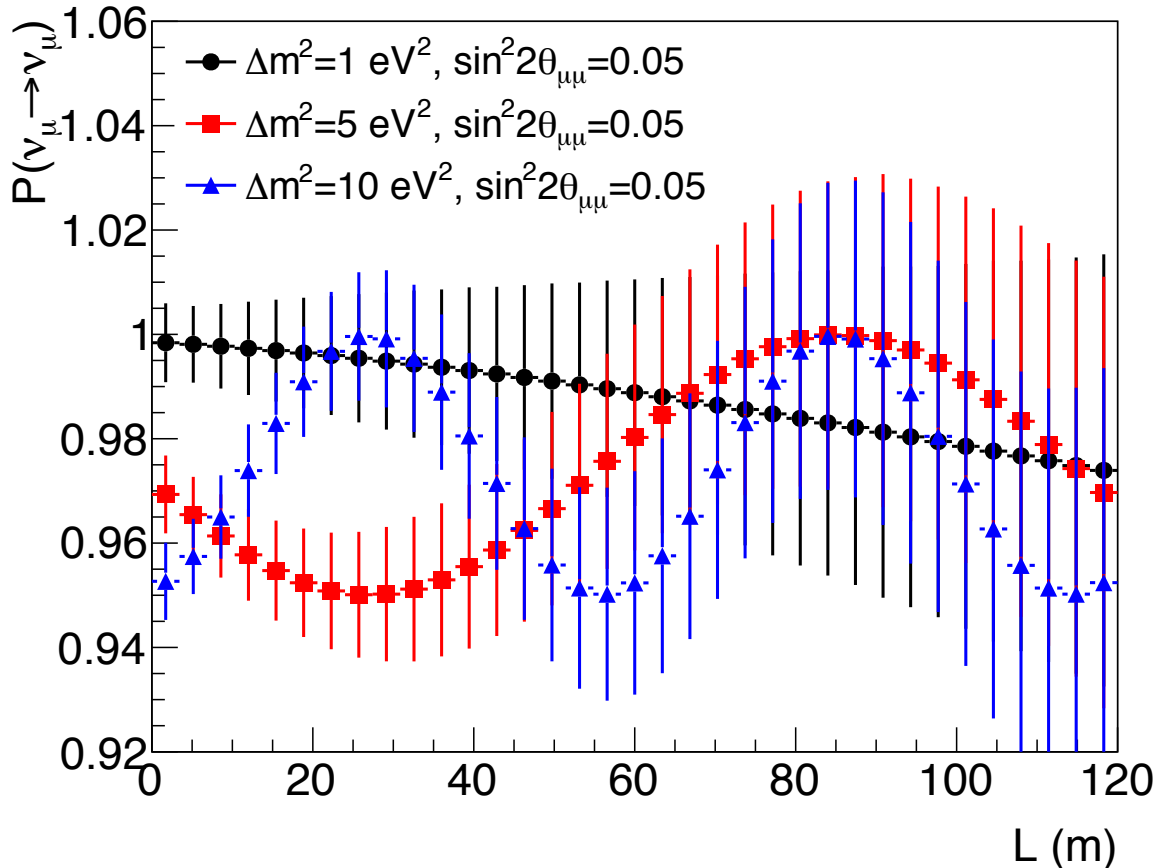


Figure 8: Three sample oscillation probability measurements as a function of L/E for 3 years of running. The error bars incorporate statistical uncertainties of both the ν_μ signal and the cosmic ray background.

5 Sensitivity

The expected number of ν_μ events in the KPipe detector as a function of distance is calculated in two steps. First, we assume the entire fiducial volume is located an arbitrary distance away from the neutrino source and determine the expected number of events based on the cross-section, ν_μ production rate, detector up-time, and total efficiency, shown in Table 1. Then, each event is weighted by the arbitrary distance squared divided by the distance to a random point in the detector squared. This gives the expected number of events as a function of distance given a no-oscillation hypothesis. At every distance along the detector, the ν_μ events are then re-scaled according to the disappearance probability (Equation 3). The oscillation probabilities for three different Δm^2 values (1, 5, 10 eV^2) can be seen in Fig 8. The error bars correspond to the statistical uncertainty associated with a 3 year ν_μ measurement with a CR rate of 27 Hz. This background rate corresponds to 132 CR events that pass our selection cuts for each 1 m slice of the detector.

The sensitivity of the experiment is evaluated using a shape-only χ^2 statistic

similar to that described in Ref. [56]. However, we replace the covariance matrix with the Neyman χ^2 convention, since we do not include any correlated systematic uncertainties between each L/E bin. Using Eq. 3 for the oscillation probability, the χ^2 value at each pair of oscillation parameters, Δm^2 and $U_{\mu 4}$, is calculated by comparing the no-oscillation signal ($N_i^{\nu, \text{un}} + N_i^{\text{bkgd}}$) to the oscillation signal ($N_i^{\nu, \text{osc}} + N_i^{\text{bkgd}}$) in each L/E bin, i . Here, $N_i^{\nu, \text{un}}$ and $N_i^{\nu, \text{osc}}$ are defined as the number of expected ν_μ events in bin i given a no-oscillation prediction and an oscillation prediction, respectively. The number of events in a bin due to background is then added to the ν_μ prediction. The ΔL value used in setting the bin size is 0.5 m. Defining for each i^{th} L/E bin the difference between the no-oscillation and oscillation signal, n_i , where

$$n_i = \left(N_i^{\nu, \text{un}} + N_i^{\text{bkgd}} \right) - \left(\xi N_i^{\nu, \text{osc}} + N_i^{\text{bkgd}} \right), \quad (4)$$

the χ^2 is then

$$\chi^2 = \sum_i^{\text{nbins}} \frac{n_i^2}{N_i^{\nu, \text{un}} + N_i^{\text{bkgd}}}. \quad (5)$$

The normalization constant, ξ , in Eq. 4, is included in order to make the analysis shape-only and is constrained to be

$$\xi = \frac{\sum_i N_i^{\nu, \text{un}}}{\sum_i N_i^{\nu, \text{osc}}}. \quad (6)$$

For the 90% confidence limit reported, a one degree of freedom, one-sided raster scan threshold of $\chi^2 = 1.64$ is used. The 5σ threshold is $\chi^2 = 25.0$, considering a one degree of freedom, two-sided raster scan.

Parameter	Value
Detector length	120 m
Detector fiducial radius	1.45 m
Closest distance to source	32 m
Liquid scintillator density	0.863 g/cm ³
Active detector mass	684 tons
Proton rate (1 MW)	3.75×10^{22} POT/year
KDAR ν_μ yield (MARS15)	0.0072 ν_μ /POT
ν_μ CC σ @ 236 MeV (NuWro)	1.3×10^{-39} cm ² /neutron
Raw KDAR CC event rate	1.02×10^5 events/year
KDAR signal efficiency	77%
Vertex resolution	80 cm
Light yield	4500 photons/MeV
ν_μ creation point uncertainty	25 cm
Cosmic ray background rate	27 Hz

Table 1: Summary of the relevant experimental parameters.

For the subsequent sensitivity plots, the oscillation prediction, $N_1^{\nu, \text{osc}}$, has been simplified by the two flavor approximation to the 3+1 neutrino oscillation model (Equation 3), where we define $\sin^2(2\theta_{\mu\mu}) = 4|U_{\mu 4}|^2(1 - |U_{\mu 4}|^2)$.

The KPipe search for sterile neutrinos, which uses only the relative rate of events along the pipe, is helped by the fact that uncertainties associated with the absolute normalization of the event rate expectation are not relevant for this shape-only analysis. This includes theoretical uncertainties in the kaon production and neutrino cross section. Instead, the dominant uncertainty associated with the weight of each bin comes from the combined statistical uncertainty of the ν_μ measurement and the CR background. In the sensitivity studies, we assume a CR background rate of 27 Hz over the entire detector. Further, there are two uncertainties associated with the neutrino baseline L : the creation point of the ν_μ from the decaying K^+ has a linear uncertainty of 25 cm; the reconstructed position resolution, described in Section 4, has a Gaussian uncertainty of 80 cm. There is no uncertainty associated with the energy reconstruction since the ν_μ have a definite energy. We also include a total detection efficiency due to the selection cuts, dead-time, and escaping muons described in Section 4.1 of 75%. A summary of the relevant experimental parameters and assumptions can be seen in Table 1.

Fig. 9 shows the projected 90% and 5σ sensitivity of KPipe to $\nu_\mu \rightarrow \nu_\mu$ for 3 years of running. The global fit allowed regions, given in red, were produced using a new software package based on the previous work of Ignarra *et al.* [13]. We refer to this work as “Collin *et al.*” [57]. The fit includes the datasets described in Ref. [58] with the exception of the atmospheric limit. The model parameters are explored using a Markov chain Monte-Carlo algorithm. Contours are drawn in a two-dimensional parameter space using 2 degree of freedom χ^2 values for 90% and 99% probability. After 3 years of KPipe running, the 5σ exclusion contour covers the best fit point at $\Delta m^2 = 0.93 \text{ eV}^2$ and $\sin^2(2\theta_{\mu\mu}) = 0.11$.

5.1 KPipe sensitivity versus past results and future experiments

Fig. 10 compares KPipe’s predicted six year 90% sensitivity to current experimental limits and to the predicted sensitivity of the future Short Baseline Neutrino (SBN) experiment that will take place at Fermilab [31]. All contours are for 90% CL. Contours that are solid are for experiments that use only shape information, while dashed contours are used for experiments utilizing both shape and rate information.

Kpipe’s sensitivity above $\Delta m^2 > 1 \text{ eV}^2$ extends in the mixing angle about an order of magnitude further than the muon neutrino disappearance limits from Super-K [59] and the combined results from MiniBooNE and SciBooNE. Below 1 eV^2 , where KPipe’s sensitivity becomes limited, the parameter space has begun to be explored by the latest sterile search from Ice Cube, which looked for muon- and anti-muon to sterile disappearance of atmospheric neutrinos [60]. Such oscillations would come from the MSW resonance effect as the neutrinos passed through the Earth’s core. With the addition of KPipe, much of the muon disappearance parameter space will have been explored.

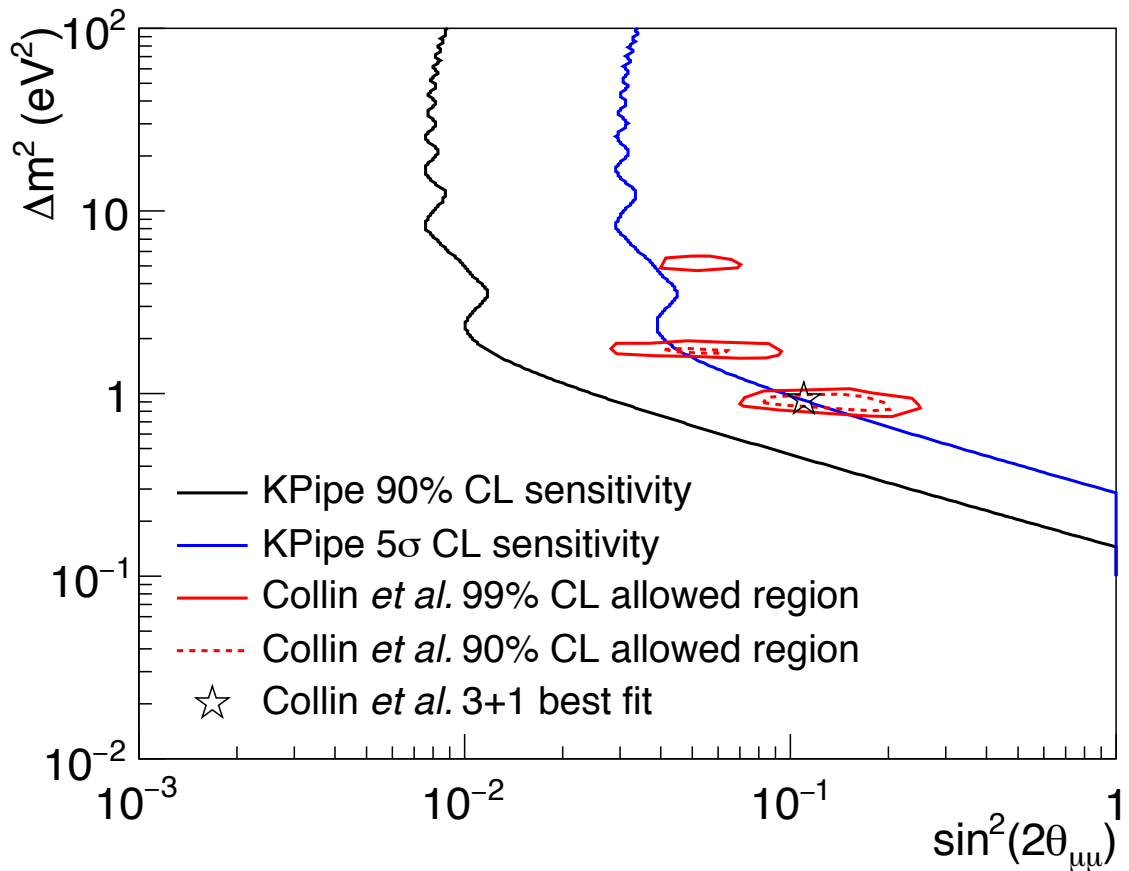


Figure 9: The projected sensitivity of KPipe to muon neutrino disappearance with 3 years of running, including the cosmic ray background, signal efficiencies, and reconstruction uncertainties described in the text. The red contours are the global allowed regions given by Collin *et al.* [57].

SBN and KPipe have similar sensitivity reach in the $\Delta m^2 = 1 - 4 \text{ eV}^2$ region. The SBN program consists of three detectors that will be combined to search for short baseline oscillations. The SBN contour assumes that the detectors get 6.6×10^{20} POT (3 years) of data for two of the detectors, SBND and the ICARUS-T600, and 13.2×10^{20} POT (6 years) for the third detector, MicroBooNE. SBN performs better at low- Δm^2 and KPipe at high- Δm^2 ; the complementarity between the experiments is clear.

6 Cost Estimate

In this section, the estimated cost of the KPipe detector components are presented.

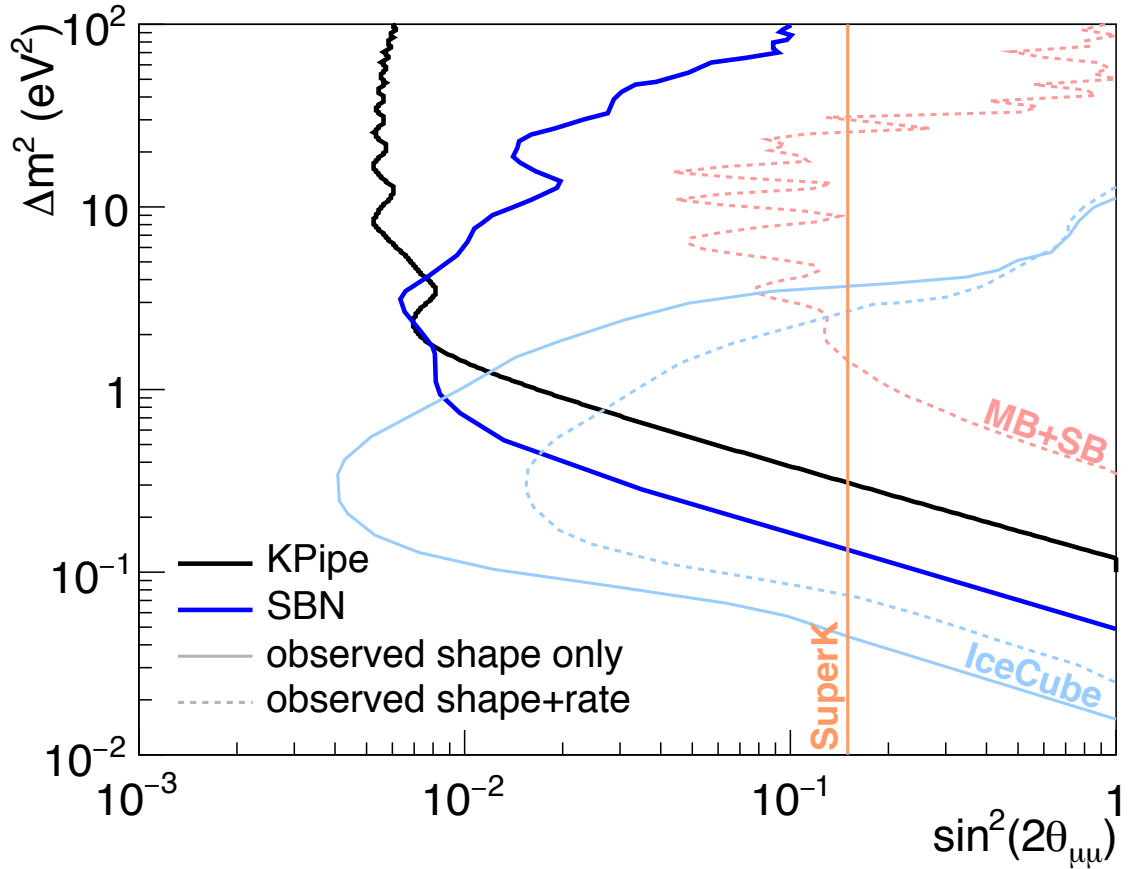


Figure 10: The 90% CL sensitivity of KPipe with 6 years of running (in black), compared to the 90% CL limit or sensitivity of past, current, and future experiments. This includes limits from a combined MiniBooNE and SciBooNE analysis (in red), Super-K (in orange), and IceCube in (light blue). The sensitivity of the future SBN experiment is shown in dark blue. Results from shape-only measurements are shown as solid contours. The dashed contours come from rate and shape measurements. The sensitivity contours for the future SBN program are for 6 years of MicroBooNE data combined with 3 years of SBND and ICARUS data. The KPipe sensitivity estimate includes the cosmic ray background, signal efficiencies, and reconstruction uncertainties described in the text.

6.1 Vessel

Contech Engineered Solutions supplies a High-Density Polyethylene (HDPE) pipe that has been used for chemical storage underground. These pipes are also typically used for irrigation or drainage. It is reinforced radially with steel rods to maintain its circular shape, while flexible longitudinally for thermal expansion or flexibility in the event of an earthquake. We believe the HDPE will be compatible with various types of liquid scintillators. Due to the compatibility with liquid scintillator, ease of construction, and safety, we expect HDPE to be suitable for KPipe.

The cost of the vessel, the 120 m, 2.995 m inner diameter HDPE pipe, including two bulkheads and two 30" risers for cabling, comes to approximately \$288,000. The full field, electro-fusion welding services to assemble the vessel was quoted at approximately \$54,000, with an extra \$5,500 for leak testing the vessel. We also require an overflow tank capable of storing approximately 0.3% of the total LS volume. This adds an extra \$16,000 including bulkheads and a stub to connect a line to the main vessel.

6.2 Scintillator

We are currently considering using a mineral oil based liquid scintillator similar to that used in the NOvA experiment. Approximately 95% by mass is the mineral oil, which acts as a solvent, and the remaining 5% is mostly pseudocumene, which is the scintillator. Trace amounts of PPO and bis-MSB are also added. These act to downshift the UV photons to longer wavelengths (~ 420 nm) where the quantum efficiencies of typical photodetectors are maximal. The cost of mineral oil and pseudocumene is strongly related to the market price of oil. This will be the largest uncertainty when determining when to acquire the liquid scintillator. KPipe requires a total of 732 tons of the NOvA scintillator mixture. Based on NOvA's estimate as to the cost of their scintillator, \$1.53M/kiloton [61][62], we expect the scintillator for KPipe to cost approximately \$1.1 M.

We have the ability to increase the light yield by changing the pseudocumene content or by using a different liquid scintillator, such as Linear Alkylbenzene (LAB). A higher light yield could allow us to reduce the number of SiPMs (which are the dominant cost driver). However, other scintillators will likely be more expensive than the mineral oil mixture.

6.3 Photon detectors and Readout Electronics

The light collection system is designed to have hoops of SiPMs, which are separated by 10 cm lengths along the axis of the detector (1200 hoops). These hoops are mounted on panels, which optically separate the fiducial region from the veto region. A single hoop contains 100 SiPMs and is read out on a single channel. Based on the reflective panels used in the MiniBooNE experiment, we expect the panels to cost approximately \$150/m². With this design, KPipe will require 120,000 SiPMs and 1200 readout channels for the fiducial volume. The design of the veto currently calls for an additional 1200 SiPMs – attached to 120 hoops – and a total of 12 readout channels. We have received quotes from two separate companies (Hamamatsu, SenSL) regarding the price of SiPMs and expect to be able to purchase them in bulk for \$15-20 per SiPM. Each channel, including cabling, data acquisition, and readout, will cost approximately \$300.

6.4 Facilities

In our cost estimates, we do not include the cost of civil construction for any on-site modifications to the MLF grounds. To install the detector, a 120 m trench dug out

radially from the target station 5 m deep will need to be made. Burying KPipe has the benefits of introducing a slight overburden to help shield against cosmic rays and of insulating the detector from daily temperature fluctuations. If the detector is installed at the location specified in the paper, KPipe will require removing a 5 m section of the road, tree removal, and modifying the location of a storage tank located outside the western wall of the MLF. Once the HDPE components are electro-fusion welded in place, the trench can be filled and the road can be repaired. A small concrete storage building will have to be built to house the electronics and the expansion tank. Once the experiment is complete, the tank can be dug up, the trench refilled, and the trees replanted.

An alternative to burying the KPipe detector would be to house the pipe above ground in a long concrete structure whose internal air temperature is controlled. This avoids digging a trench. However, it will require rerouting the road behind the MLF building.

6.5 Cost Summary for Detector

Component	Quantity	Unit price [\$M/unit]	Total [\$M]
Vessel Pipe	120 m	0.0024/m	0.288
Vessel Risers	2	0.00065/riser	0.0013
Pressure Tests	1	0.0055/test	0.0055
Expansion Tank	1	0.016/tank	0.016
SiPMs	132200	0.00002/SiPM	2.644
Readout Channels	1322	0.0003/channel	0.3966
Paneling	1056 m ²	0.00015/m ²	0.158
Scintillator	0.732 ktons	1.5/kton	1.1
Total			4.6

Table 2: Summary of component costs. The total estimated cost of the KPipe detector is \$4.6 million.

7 Estimated Schedule

KPipe is designed with components that are well-established in order to be able to minimize the cost and time of engineering and construction, while still accomplishing its physics goals.

The first two years of the experiment would be dedicated to the construction of the different components: the tank and SiPM hoops, the readout electronics, the scintillator, and trench. This can proceed in parallel:

- One subset of the participating institutions take one year to do the mechanical engineering for the pipe, the internal structure to optically separate the inner from the veto volume, and the SiPM hoops. Once this is completed, they will commence with the construction and testing of the SiPM hoops.

Tasks	year 1	year 2	year 3	year 4	year 5	year 6	year 7	year 8	year 9	year 10
Engineering of vessel	■	■								
Design of SiPM hoops	■	■								
Testing and construction of SiPM hoops			■	■						
Design and assembly of readout electronics	■	■	■	■						
Production of scintillator	■	■	■							
Trench planning and construction	■	■	■	■						
Ship components to J-PARC for assembly of vessel				■						
Commissioning					■					
Data Taking						■	■	■	■	■

Figure 11: Estimated schedule from beginning of construction to the completion of the physics data run.

- Another subset of institutions will be responsible for assembling the readout electronics. They will order components, build the boards, and perform quality control.
- The other subset would be responsible for acquiring the precursors of the scintillator. They will produce batches and test the scintillator.
- During this time, the excavation of the trench for the pipe will begin.

Once the components above are ready, the institutions would send them to J-PARC to be assembled together into the full detector. We estimate that this would take about a year. Once assembled a period of several months would be required to commission the detector. This would be followed by a first run of three years of physics data taking. With this data, we would have the sensitivity cover the parameter space favored by global fits to 5σ . After a total of six years of data, we expect to be able to further the limits on ν_μ disappearance by an order of magnitude. Figure 11 shows a chart outlining the estimated schedule.

8 Conclusion

The J-PARC MLF facility provides a unique and intense source of neutrinos in the form of monoenergetic 236 MeV muon neutrinos coming from the decay-at-rest of positively charged kaons. The KPipe experiment seeks to take advantage of this source for a decisive ν_μ disappearance search at high- Δm^2 in order to address the existing anomalies in this parameter space. The 120 m long, 3.0 m diameter liquid scintillator based active volume (684 ton) will feature 0.4% photo-coverage for detecting these ν_μ CC events in an attempt to discern an oscillation wave along the length of the detector.

In contrast to other neutrino sources, the KPipe neutrinos are dominantly monoenergetic. This provides a great advantage in searching for neutrino oscillations.

A neutrino (or antineutrino) induced double-coincidence muon signal detected with KPipe has a 98.5% chance of being from a 236 MeV ν_μ CC event. This simple fact allows the active detector requirements to be extremely modest, the systematic uncertainties to be practically eliminated, and the detector's energy resolution to be only a weak consideration.

Within three years of running, KPipe will be able to cover the current global fit allowed region to 5σ . The sensitivity for a 6 year run at the J-PARC facility will enhance existing single experiment limits on ν_μ disappearance by an order of magnitude in Δm^2 . Such a measurement, when considered alone, but especially in combination with existing and proposed electron flavor disappearance and appearance measurements, can severely constrain models associated with oscillations involving one or more light sterile neutrinos.

References

- [1] A. Aguilar *et al.* [LSND Collaboration], Phys. Rev. D **64**, 112007 (2001).
- [2] A.A. Aguilar-Arevalo *et al.* [MiniBooNE Collaboration], Phys. Rev. Lett. **110**, 161801 (2013).
- [3] A.A. Aguilar-Arevalo *et al.* [MiniBooNE Collaboration], Phys. Rev. Lett. **102**, 101802 (2009).
- [4] G. Mention, M. Fechner, T. Lasserre, T.A. Mueller, D. Lhuillier, M. Cribier and A. Letourneau, Phys. Rev. D **83**, 073006 (2011).
- [5] C. Zhang, X. Qian, and P. Vogel, Phys. Rev. D **87**, 073018 (2013).
- [6] M.A. Acero, C. Giunti and M. Laveder, Phys. Rev. D **78**, 073009 (2008).
- [7] C. Giunti and M. Laveder, Phys. Rev. C **83**, 065504 (2011).
- [8] J.N. Abdurashitov *et al.* [SAGE Collaboration], Phys. Rev. C **80**, 015807 (2009).
- [9] F. Kaether, W. Hampel, G. Heusser, J. Kiko and T. Kirsten, Phys. Lett. B **685**, 47 (2010).
- [10] S. Axani *et al.* Phys. Rev. D **92**, 092010 (2015).
- [11] S. Axani *et al.*. <http://dspace.mit.edu/handle/1721.1/98388> (2015).
- [12] M. Sorel, J.M. Conrad and M. Shaevitz, Phys. Rev. D **70**, 073004 (2004).
- [13] J.M. Conrad, C.M. Ignarra, G. Karagiorgi, M.H. Shaevitz and J. Spitz, Adv. High Energy Phys. **2013**, 163897 (2013).
- [14] J. Kopp, P.A.N. Machado, M. Maltoni and T. Schwetz, JHEP **1305**, 050 (2013).
- [15] C. Giunti and M. Laveder, Phys. Lett. B **706**, 200 (2011); Phys. Rev. D **84**, 073008, (2011).

- [16] B. Armbruster *et al.* [KARMEN Collaboration], Phys. Rev. D **65**, 112001 (2002).
- [17] G. Cheng *et al.* [MiniBooNE and SciBooNE Collaborations], Phys. Rev. D **86**, 052009 (2012).
- [18] J.M. Conrad and M.H. Shaevitz, Phys. Rev. D **85**, 013017 (2012).
- [19] K.B.M. Mahn *et al.* [SciBooNE and MiniBooNE Collaborations], Phys. Rev. D **85**, 032007 (2012).
- [20] P. Adamson *et al.*, [MiniBooNE Collaboration], Phys. Rev. Lett. **102**, 211801 (2009).
- [21] P. Astier *et al.* [NOMAD Collaboration], Phys. Lett. B **570**, 19 (2003); D. Gibin, Nucl. Phys. Proc. Suppl. **66**, 366 (1998); V. Valuev [NOMAD Collaboration], J. High Energy Phys., Conference Proceedings, PRHEP-hep2001/190 (2001).
- [22] I. Stockdale *et al.* [CCFR Collaboration], Phys. Rev. Lett. **52**, 1384 (1984), Z. Phys. C **27**, 53 (1985).
- [23] F. Dydak *et al.*, Phys. Lett. B **134**, 281 (1984).
- [24] M. Maltoni, T. Schwetz, M.A. Tortola and J.W.F. Valle, New J. Phys. **6**, 122 (2004).
- [25] K. Abazajian *et al.*, arXiv:1204.5379 [hep-ph] (2012).
- [26] A. Bungau *et al.*, Phys. Rev. Lett. **109**, 141802 (2012).
- [27] J. Ashenfelter *et al.*, arXiv:1309.7647 [physics.ins-det] (2013).
- [28] C. Lane *et al.*, arXiv:1501.06935 [physics.ins-det] (2015).
- [29] G. Bellini *et al.*, JHEP **1308**, 038 (2013).
- [30] M. Harada *et al.*, arXiv:1310.1437 [physics.ins-det] (2013).
- [31] R. Acciarri *et al.*, [ICARUS-WA104, LAr1-ND, and MicroBooNE Collaboration] arXiv:1503.01520 [physics.ins-det] (2015).
- [32] A.J. Anderson *et al.*, Phys. Rev. D **86**, 013004 (2012).
- [33] M. Elnimr *et al.*, arXiv:1307.7097 [physics.ins-det] (2013).
- [34] J.M. Conrad and M.H. Shaevitz, Phys. Rev. D **89**, 057301 (2014).
- [35] J. Beringer *et al.* [Particle Data Group], Phys. Rev. D **86**, 010001 (2012).
- [36] J. Spitz, Phys. Rev. D **85**, 093020 (2012).
- [37] J. Spitz, Phys. Rev. D **89**, 073007 (2014).
- [38] J-PARC Project Newsletter special issue, May 2015.

- [39] D. Ayres *et al.* [NO ν A Collaboration], arXiv:hep-ex/0503053 (2005).
- [40] S. Mufson *et al.*, arXiv:1504.04035 [physics.ins-det] (2015).
- [41] Saint-Gobain. http://www.crystals.saint-gobain.com/Liquid_scintillators.aspx (2015)
- [42] H.M. O’Keeffe, E. O’Sullivan, and M.C. Chen, Nucl. Instr. Meth. A **640**, 119 (2011).
- [43] H.W.C. Tseung, J. Kaspar, and N. Tolich, Nucl. Instr. Meth. A **654**, 318 (2011).
- [44] S. Agostinelli *et al.*, Nucl. Instr. Meth. A **506**, 250 (2003). Geant4 version 4.9.6p04 is used with the QGSP_BERT physics list.
- [45] N.V. Mokhov, FERMILAB-FN-628 (1995); O.E. Krivosheev and N.V. Mokhov, “MARS Code Status”, Fermilab-Conf-00/181 (2000); O.E. Krivosheev and N.V. Mokhov, “Status of MARS Code”, Fermilab-Conf-03/053 (2003); N.V. Mokhov, K.K. Gudima, C.C. James *et al.*, “Recent Enhancements to the MARS15 Code”, Fermilab-Conf-04/053 (2004). MARS1514 is used with the LAQGSM model.
- [46] K.K. Gudima, N.V. Mokhov, and S.I. Striganov, Fermilab-Conf-09-647-APC (2009).
- [47] C. Juszczak, Acta Phys. Polon. B **40**, 2507 (2009); T. Golan, C. Juszczak, and J. Sobczyk, Phys. Rev. C **86**, 015505 (2012). NuWro version “11q” is used with a spectral function implementation.
- [48] M. Harada *et al.*, arXiv:1502.02255 [physics.ins-det] (2015).
- [49] M. Martini, M. Ericson, G. Chanfray, and J. Marteau, Phys. Rev. C **80**, 065501 (2009);
- [50] M. Martini, M. Ericson, and G. Chanfray, Phys. Rev. C **84**, 055502 (2011).
- [51] Private communication with M. Martini.
- [52] C. Andreopoulos *et al.*, [GENIE Collaboration] Nucl. Instr. Meth. A **614**, 87 (2010).
- [53] Available at <https://github.com/rat-pac/rat-pac>.
- [54] C. Haggmann, D. Lange, J. Verbeke, and D. Wright, UCRL-TM-229453 (2012).
- [55] SensL, Series-C Datasheet <http://www.sensl.com/downloads/ds/DS-MicroCseries.pdf> (2015).
- [56] A.J. Franke, Searching for Reactor Antineutrino Flavor Oscillations with the Double Chooz Far Detector. Diss. Columbia University, 2012.
- [57] G. Collin, J. Conrad, and M. Shaevitz, “Global sterile neutrino fits”, in preparation for submission to Phys. Rev. D.

- [58] C.M. Ignarra, Nuclear Physics B (Proc. Suppl.) **237**, 173 (2013).
- [59] Abe, K. et al. [LSND Collaboration] Phys. Rev. D **91**, 052019 (2015)
- [60] Jones, BJPJ. "Sterile Neutrinos in Cold Climates" Doctoral Thesis (2015)
<http://lss.fnal.gov/archive/thesis/2000/fermilab-thesis-2015-17.pdf>
- [61] H. Nicholson, Water Based Liquid Scintillator Workshop (2010)
https://math.temple.edu/~cmarloff/scint_conf/Nicholson.pdf
- [62] J. Cooper, "Cost and Schedule Status Risks and Mitigations." IPR Mini-Review (2012) http://www-nova.fnal.gov/reviews_summer_2012/FINAL%20Cost%20&%20Schedule%20Status%20and%20Risk%20&%20Mitigation%20Strategy%20for%2014Aug2012%20IPR%20mini-Review.pdf